



Published in final edited form as:

*Nanomedicine*. 2012 May ; 8(4): 440–451. doi:10.1016/j.nano.2011.07.011.

## Curcumin-loaded $\gamma$ -cyclodextrin liposomal nanoparticles as delivery vehicles for osteosarcoma

Santosh S. Dhule, MS<sup>a,b</sup>, Patrice Penfornis, MS<sup>b</sup>, Trivia Frazier, BS<sup>b</sup>, Ryan Walker, BS<sup>b</sup>, Joshua Feldman, BS<sup>b</sup>, Grace Tan, PhD<sup>a</sup>, Jibao He, PhD<sup>c</sup>, Alina Alb, PhD<sup>d</sup>, Vijay John, DEngSc<sup>a</sup>, and Radhika Pochampally, PhD<sup>b,e,\*</sup>

<sup>a</sup>Department of Chemical and Biomolecular Engineering, Tulane University, New Orleans, Louisiana

<sup>b</sup>Tulane Center for Stem Cell Research and Regenerative Medicine, Tulane University Health Sciences Center, New Orleans, Louisiana

<sup>c</sup>Coordinated Instrumentation Facility, Tulane University, New Orleans, Louisiana

<sup>d</sup>Department of Physics and Engineering Physics, Tulane University, New Orleans, Louisiana

<sup>e</sup>Department of Pharmacology, Tulane Medical School, New Orleans, Louisiana

### Abstract

The delivery of curcumin, a broad-spectrum anticancer drug, has been explored in the form of liposomal nanoparticles to treat osteosarcoma (OS). Curcumin is water insoluble and an effective delivery route is through encapsulation in cyclodextrins followed by a second encapsulation in liposomes. Liposomal curcumin's potential was evaluated against cancer models of mesenchymal (OS) and epithelial origin (breast cancer). The resulting 2-Hydroxypropyl- $\gamma$ -cyclodextrin/curcumin - liposome complex shows promising anticancer potential both in vitro and in vivo against KHOS OS cell line and MCF-7 breast cancer cell line. An interesting aspect is that liposomal curcumin initiates the caspase cascade that leads to apoptotic cell death in vitro in comparison with DMSO-curcumin induced autophagic cell death. In addition, the efficiency of the liposomal curcumin formulation was confirmed in vivo using a xenograft OS model. Curcumin-loaded  $\gamma$ -cyclodextrin liposomes indicate significant potential as delivery vehicles for the treatment of cancers of different tissue origin.

**From the Clinical Editor**—Curcumin-loaded  $\gamma$ -cyclodextrin liposomes were demonstrated in vitro to have significant potential as delivery vehicles for the treatment of cancers of mesenchymal and epithelial origin. Differences between mechanisms of cell death were also evaluated.

### Keywords

Apoptosis; Autophagy; Curcumin; Cyclodextrin; Liposome; Osteosarcoma

---

Curcumin, the constituent of *Curcuma longa* (turmeric), is known for its potent antineoplastic activity against a number of tumors, including prostate, breast and colon

---

\*Corresponding author: Tulane Center for Stem Cell Research and Regenerative Medicine, Tulane University Health Sciences Center, SL-99, New Orleans, LA 70112, USA. rpocham@tulane.edu (R. Pochampally).

cancer.<sup>1</sup> The chemopreventive efficacy of curcumin in almost all stages of carcinogenesis has received significant attention because of its low nonspecific toxicity to normal cells. Curcumin is shown to have concentration-dependent pleiotropic effects on cells; low concentrations of curcumin protect hepatocytes but higher concentrations are hepatocytotoxic.<sup>2,3</sup> The differential effect of curcumin on tumor cells versus normal cells is also attributed to the rate of curcumin uptake, which has been found to be significantly higher in tumor cells than the uptake rate in normal cells.<sup>4</sup> The widespread clinical application of curcumin has been limited due to its poor aqueous solubility and low systemic bioavailability. Reports to date indicate extremely low levels (22 – 41 ng/ml) of curcumin in serum even after high amounts (8 g/day) of oral administration, explained by its low water solubility (11 ng/ml).<sup>5–8</sup> Conjugates of curcumin with macromolecules, nano-formulations, cyclodextrins (CDs), liposomes and hydrogels have been studied to enhance water solubility, thereby increasing its circulation time and bioavailability.<sup>6</sup> For example, systemic administration of liposomal curcumin has shown an increase in bioavailability and shown a tumor-suppressing effect in various cancers.<sup>7–10</sup>

The anticancer potential of curcumin against osteosarcoma (OS) has not been fully explored and is of potentially significant impact in drug delivery. OS usually develops during the period of rapid growth in adolescence, and it occurs as a second malignant neoplasm due to a genetic predisposition and/or as a consequence of prior cancer therapy.<sup>11</sup> The incidence rates in the United States peak in adolescence and in elder years and accounts for about 60% of primary malignant bone tumors diagnosed in the first 2 decades of life. The prognosis for OS is poor, with a survival rate of 62% at 5 years (ages 0 – 24) for localized OS, and worse for metastatic disease situations.<sup>12</sup> The preferred mode of therapy is tumor removal followed by chemotherapy or radiation therapies that are nonspecific and toxic to normal cells. One of the limitations of current therapeutic options is the lack of specific therapy with fewer side effects. Therefore, there is a need to develop novel and less toxic therapeutic options to increase the cytotoxic effects. Although Walter et al have reported curcumin's cytotoxic effects on OS cell lines,<sup>13</sup> this is the first report of liposomal curcumin delivery for osteosarcoma.

CDs and liposomes have been used in recent years as drug-delivery vehicles, improving the bioavailability and therapeutic efficacy of many drugs having poor water solubility.<sup>14</sup> The amount of lipophilic drug incorporated into the conventional liposome bilayer is often limited in terms of drug-to-lipid ratio. The approach of combined use of CDs and liposomes represents a novel system of drug-in-CD-in-Liposome (DCL) preparation in drug delivery.<sup>15</sup> This article reports the preparation, characterization and evaluation of the antitumor potential of curcumin-loaded liposomal nanoparticles (NPs) in vitro and in vivo. First, we evaluated the most effective curcumin formulation against cancer of mesenchymal (KHOS and RFOS) and epithelial origin (MCF-7). Second, we looked at the apoptosis/autophagy process induced by curcumin in the different formulations tested and then evaluated curcumin liposomes in vivo. Recent literature regarding the study of PEGylated gold NPs indicates that particles smaller than 100 nm are able to penetrate the tumor vasculature effectively.<sup>16</sup> The observations imply that the added flexibility of soft liposomal systems in this size range should enable such penetration and uptake into cells through endocytosis. Our objective is therefore to prepare liposomes containing curcumin encapsulated in CDs (for

enhanced solubility) in the size range for effective delivery and to measure the efficacy of such formulations for both in vitro and in vivo studies.

## Methods

### Materials

Curcumin was obtained from Acros Organics, Morris Plains, New Jersey, and the 2-Hydroxypropyl- $\gamma$ -cyclodextrin (HP $\gamma$ CD) from Sigma-Aldrich, St. Louis, Missouri. DMPG (1, 2-dimyristoyl-sn-glycero-3-(Phospho-rac-(1-glycerol))), DPPC (1, 2-dipalmitoyl-sn-glycero-3-Phosphocholine) and Mini-Extruder were from Avanti Polar Lipids, Alabaster, Alabama. Dulbecco's Modified Eagle's Medium (DMEM),  $\alpha$ -MEM (minimum essential medium) and fetal bovine serum (FBS) were from Invitrogen, Carlsbad, California. The KHOS cell line was obtained from the American Type Culture Collection and MCF-7 was a generous gift from Dr. Brian Rowan (Tulane Cancer Center, New Orleans, Louisiana). Skin fibroblast and human mesenchymal stem cells (MSCs) were from Tulane Center for Stem Cell Research and Regenerative Medicine, New Orleans. RFOS is a primary cell line established from an untreated OS from a patient undergoing biopsy in accordance with the protocol approved by Ochsner Hospital. The tumor was located in the proximal humerus. The RFOS cell line was derived according to the protocol described in DeComas et al.<sup>17</sup>

### Preparation of conventional curcumin liposomes

Conventional curcumin liposomes (CD-free liposomes) were prepared by thin-film evaporation.<sup>8,18</sup> Curcumin and phospholipids were mixed in the ratio of about 1:10 (w/w). The 2 phospholipids, DPPC and DMPG, were mixed in the ratio 1:1 (w/w). Curcumin (0.013 g) and phospholipid (0.05 g each) were dissolved in 10 ml of chloroform and methanol mixture (2:1 v/v). The solution was evaporated by using a rotary evaporator for 2.5 hours to form a dry lipid film. The lipid film was then hydrated for 1 hour with 5 ml of 1X PBS at 50 °C and 125 rpm. The hydrated solution was extruded 11 times through a 400 nm polycarbonate membrane at 50 °C followed by the use of a 100-nm membrane from Whatman, Mobile, Alabama. Empty liposomes were prepared using the same protocol but excluding curcumin. The empty (curcumin-free) liposomes were used as a control to study the effect of phospholipids on all cell lines. The structures of the phospholipids and curcumin are provided in the Supplementary Materials.

### Entrapment of HP $\gamma$ CD-curcumin complex into liposomes

HP $\gamma$ CD-curcumin liposomes were prepared by using the protocol described for conventional curcumin liposomes with a small variation in the contents of the hydration medium. Conventional curcumin liposomes were made using PBS as a hydration solution, and curcumin was incorporated into the dried phospholipid film before hydration. For the HP $\gamma$ CD-curcumin system, the PBS buffer additionally contained the HP $\gamma$ CD-curcumin complex. The HP $\gamma$ CD-curcumin system was made using the following steps. First, 0.125 g (2.5%) HP $\gamma$ CD was dissolved in 5 ml PBS and excess curcumin was added to the above mixture. The concentration of HP $\gamma$ CD was optimized in the range of 0 to 11 % of HP $\gamma$ CD. The HP $\gamma$ CD-curcumin mixture in PBS was heated at 50 °C for 2.5 hours. The supernatant containing the HP $\gamma$ CD-curcumin inclusion complex was separated from the insoluble excess

curcumin by centrifugation at 2000 g for 10 minutes. This aqueous HP $\gamma$ CD-curcumin inclusion complex was used during the hydration step that results in entrapment of the HP $\gamma$ CD-curcumin complex inside the liposomes.<sup>19</sup>

### **Cryo-TEM and DLS**

A drop of liposome suspension was placed on a Formvar-coated copper TEM grid. The grid was blotted to form a thin film and rapidly vitrified in liquid ethane. The vitrified specimens were transferred, under liquid nitrogen, to a JEOL 2011 microscope equipped with a Gatan cold stage, and examined under acceleration voltage of 120 kV in conventional TEM mode. The temperature of the sample grid was maintained at  $-175\text{ }^{\circ}\text{C}$  during the course of imaging.<sup>20</sup> The diameter of the liposomes was measured from the cryo-transmission electron microscopy (cryo-TEM) images using Advanced Microscopy Techniques (AMT) camera software version 4.1. The size distributions of the liposomal formulations were characterized using a dynamic light scattering (DLS) instrument (90Plus particle size analyzer - Brookhaven Instruments Corporation, Holtsville, New York) at a wavelength of 670 nm and 90-degree detection angle.<sup>21,22</sup>

### **Encapsulation efficiency of liposomal curcumin**

One milliliter of liposomal curcumin solution was added to a Quick-Seal centrifuge tube of size 13  $\times$  38 mm and capacity 3.9 ml. Samples were spun down at 100,000 g for 1.5 hours on Beckman Coulter ultracentrifuge, Fullerton, California.<sup>23</sup> Curcumin in supernatant and pellet was quantified. The encapsulation efficiency defined as % encapsulation =  $(C_l/C_T) \times 100$ , where  $C_l$  – curcumin in liposome,  $C_T$  – total curcumin in the liposome preparation, was used in calculation.

### **Quantification of liposomal curcumin**

Liposomal curcumin was quantified by a colorimetric assay.<sup>18</sup> A standard curve was formulated from known concentrations of curcumin in DMSO and diluted in lysis buffer HBSE-Triton X-100 (10 mM HEPES, 140 mM NaCl, 4 mM EDTA, 1% Triton X-100). Liposomal curcumin samples were incubated for 5 minutes in lysis buffer and then absorbance was measured at 450 nm on a Fluostar Optima microplate reader (Labtech, Inc., Durham, North Carolina).

### **Cell culture**

Cancer cell lines KHOS, RFOS and MCF-7 were grown in DMEM supplemented with 10% FBS, 100 units/ml penicillin and 100  $\mu\text{g/ml}$  of streptomycin. Human MSCs and skin fibroblast were cultured in  $\alpha$ -MEM containing 17% FBS, 100 units/ml of penicillin and 100  $\mu\text{g/ml}$  of streptomycin. Cells were maintained at  $37\text{ }^{\circ}\text{C}$  with 5%  $\text{CO}_2$  in a humidified incubator.

### **In vitro treatment of curcumin formulations**

Cells were seeded in a 96-well plate (5000 cells/well) and allowed to grow for 48 hours. Four different curcumin formulations – DMSO-curcumin, HP $\gamma$ CD-curcumin inclusion complex, conventional curcumin liposomes (CD-free) and HP $\gamma$ CD-curcumin liposomes –

were tested for their cytotoxic potential on the 96-well plates. Liposomal curcumin stocks and DMSO-curcumin were diluted to get desired concentration range from 4 to 28 µg/ml.

### Cell proliferation assay

After 48 hours of curcumin treatment, the media were removed from the plates, rinsed with PBS and the plates were frozen at  $-80^{\circ}\text{C}$  overnight. The cells were thawed at room temperature and 200 µl of CyQUANT GR dye/cell lysis buffer (Invitrogen, Carlsbad, California) was added to each well. The fluorescence was measured using a Fluostar Optima microplate reader (Ex 485 nm and Em 530 nm).<sup>24,25</sup> The mean value and standard deviation (SD) for each treatment were determined and then converted to percentage relative to control. From the data, a dose-response curve was drawn and the 50% inhibitory concentration ( $\text{IC}_{50}$ ) was determined using GraphPad Prism 5 software.<sup>26</sup>

### Western blot analysis

KHOS cells were treated with curcumin liposomes (Conventional) in the range 0 to 10 µg/ml. After 48 hours, treated cells were lysed and the lysate was subjected to western blot analysis. Briefly, cellular lysates were prepared using RIPA buffer with protease inhibitor cocktail (Santa Cruz Biotech, Santa Cruz, California). The protein content was measured with BCA assay kit (Bicinchonic Acid, Pierce, Rockford, Illinois) and 100 µg of total protein was resolved by SDS-polyacrylamide gel electrophoresis (NuPAGE, 4–12% Bis-Tris gels, Invitrogen). The sample was transferred to a PVDF membrane (Millipore, Billerica, Massachusetts). The membrane was blocked for 2 hours with PBS containing 0.05% Tween 20 and 5% nonfat dry milk (Santa Cruz Biotech) and then incubated overnight at  $4^{\circ}\text{C}$  with primary antibody (Caspases-3, -7, their cleaved forms, and PARP monoclonal antibody from Caspase detection kit, Cell Signaling Technology, Danvers, Massachusetts). The membrane was washed several times with PBS containing 0.05% Tween 20 and the bound primary antibody was detected by incubating 1 hour with horseradish peroxidase-conjugated goat anti-rabbit IgG. The membrane was washed and developed using enhanced chemiluminescence assay (ECL, Pierce).

### Detection of apoptosis and autophagy by fluorescence microscopy

KHOS cells were treated at  $\text{IC}_{50}$  concentration of different curcumin formulations and representative fields of cells were photographed after 48 hours with EVOS microscope (AMG, Mill Creek, Washington). Coverslips with adherent KHOS were washed with cold PBS and fixed with 4% paraformaldehyde after 48 hours of treatment. The specimens were then stained with Hoechst 33342 (0.5 µg/ml) in Supermount (BioGenex, San Ramon, California). Another set of KHOS cells treated in parallel was fixed in 4% paraformaldehyde and permeabilized by incubating with 0.25% Triton X-100 in PBS for 10 minutes. Slides were washed 3 times with (PBS + 0.1% BSA) for 5 minutes. Specimen was treated with blocking solution (PBS containing 0.05% Tween 20, 1% BSA and 20% goat serum) overnight. Then cells were incubated overnight at  $4^{\circ}\text{C}$  with primary antibody against beclin-1 (Abgent) diluted 1:25 in PBS and 1% BSA. After 3 washes, secondary antibody Alexafluor A555 (1:250) in PBS with 1% BSA was added and incubated for 1 hour. After several washes, slides were mounted with 10 µl of Supermount (BioGenex) containing

Hoechst 33342 (0.5 µg/ml) and observed under BD Pathway 855 high-content cell analyzer (BD Biosciences, San Jose, California).

### **Xenograft model of OS**

In vivo study has been approved by the Institutional Animal Care and Use Committee of Tulane University. Mice were regularly monitored over the period of experiment. KHOS cells were cultivated under standard conditions, prepared for injection in Hank's buffered saline solution (HBSS), and 1 million cells subcutaneously injected into immunodeficient nude mice (nu/nu strain). The tumors were allowed to develop for 3 weeks prior to treatment. Next, 20 microliters of curcumin liposomes were injected intratumorally every 48 hours during 2 weeks. The control tumors were treated with empty liposomes. The mice were euthanized following 2 weeks of treatment, or according to a veterinary advisory.

### **Colorimetric detection of apoptosis in tissue sections**

Paraffin tissue sections of tumors were rehydrated and stained with the DeadEnd™ Colorimetric TUNEL System (Promega Corporation, Madison, Wisconsin) following the manufacturer's protocol.<sup>27</sup> Sections were permeabilized 20 minutes with 20 µg/ml Proteinase K. After equilibration, samples were incubated 1 hour at 37 °C with the biotinylated nucleotide-rTdT enzyme mixture. After several washes in 2X Sodium Chloride-Sodium Citrate Buffer (SSC) and PBS, endogenous peroxidases were blocked by incubating slides 5 minutes in 0.3% hydrogen peroxide. Then slides were incubated 30 minutes at room temperature with the streptavidin-horseradish peroxidase solution and positive apoptotic-brown cells were revealed by 5 minutes incubation in 3, 3'-diaminobenzidine (DAB) solution. Slides were mounted using Supermount solution (BioGenex). Hematoxylin and eosin (HE) staining was performed on tumor tissue sections to detect the histopathology of the treated tumor. Slides were observed under EVOS inverted microscope (AMG).

## **Results**

### **Characterization and encapsulation efficacy of liposomal curcumin**

The hydrophobic nature of curcumin allows it to become incorporated into the bilayer region of the vesicles. However, this rather limits the amount of drug that can be delivered, so we have sought to encapsulate CD-solubilized curcumin within the liposomes. Curcumin is a symmetric molecule with 2 moieties, 3-methoxy 4-hydroxy substituted phenyl, which are moieties that can be enclosed in a CD cavity. By forming water-soluble complexes, HP $\gamma$ CD (2-Hydroxypropyl- $\gamma$ -cyclodextrin) increases the aqueous solubility of curcumin from 11 ng/ml to 600 µg/ml. This  $\sim 10^4$ -fold increase in water solubility allows curcumin to be accommodated in the aqueous phase of vesicles. The stoichiometry of the HP $\gamma$ CD-curcumin complex has been shown to be 2:1 as depicted in Figure 1, A.<sup>28</sup> The formation of inclusion complex of curcumin and HP $\gamma$ CD was confirmed visually by the solubilization of practically insoluble curcumin; when added to a solution of HP $\gamma$ CD, the characteristic yellow color of curcumin is observed. Cryo-TEM images (Figure 1, C and D) of conventional and HP $\gamma$ CD-curcumin liposomes illustrate highly spherical liposomes. The cryo-TEM images were taken at 2 different resolutions (Figure 1, C -15000 $\times$  and D - 12000 $\times$ ) and the magnification in Figure 1, D is accordingly adjusted to provide consistency in scale with Figure 1, C. Figure

1, D illustrates that the liposomes retain a spherical shape even after incorporation of CD. The higher magnification inset in the cryo-TEMs illustrates finer details of liposomal morphology. The size distribution analysis from DLS and cryo-TEM are reported in Table 1.

Encapsulation levels for conventional (CD-free) and HP $\gamma$ CD-curcumin liposomes were found to be 0.8 mg/ml and 1.3 mg/ml, respectively. The entrapment of curcumin increased from 30% in CD-free liposomes to 50% when the HP $\gamma$ CD host is used (Table 2). The optimum encapsulation was found at 2.5% HP $\gamma$ CD.

### Cytotoxicity study

The anticancer activity of different curcumin formulations was examined against 3 cancer cell lines. The formulations used were DMSO-curcumin, conventional curcumin liposomes, HP $\gamma$ CD-curcumin complex, and HP $\gamma$ CD-curcumin liposomes. The cancer cell lines used were KHOS, RFOS and MCF-7. KHOS and RFOS are OS cell lines of mesenchymal origin and the breast cancer cell line, MCF-7, of epithelial origin. In addition to cancer cell lines, normal human cells were evaluated as controls for cytotoxicity. MSCs were used as control for OSs and epithelial-originated skin fibroblasts were the corresponding control for the breast cancer cell line. The IC<sub>50</sub> values (Inhibitory concentration necessary to inhibit 50% of cell growth) for KHOS, MCF-7 and skin fibroblast are listed in Table 3.

As shown in Figure 2, A, all curcumin formulations have an effect on the viability of the control MSCs at higher concentrations, with IC<sub>50</sub> values greater than 25  $\mu$ g/ml. In contrast, Figure 2, B indicates that KHOS has a strong sensitivity to conventional and HP $\gamma$ CD-curcumin liposomes, with IC<sub>50</sub> value in the range of 5 – 6  $\mu$ g/ml. KHOS is a fast-growing cell line and the increased metabolism results in an increased uptake of liposomal curcumin.<sup>29</sup> Both the liposomal curcumin formulations are significantly more effective than all other formulations in affecting cell viability for KHOS.

Figure 2, C illustrates that RFOS cells are resistant to all curcumin formulations in the specified concentration range 4 to 28  $\mu$ g/ml. The cell viability of skin fibroblast was influenced by all curcumin formulations at concentrations of 20  $\mu$ g/ml except HP $\gamma$ CD-curcumin complex (Figure 2, D). The HP $\gamma$ CD-curcumin complex is not cytotoxic (except for KHOS) even at the highest concentration of 28  $\mu$ g/ml used in this study. Figure 2, E illustrates that MCF-7 viability is affected by curcumin level, and the cells are more sensitive to liposomal curcumin than DMSO-curcumin. The IC<sub>50</sub> of liposomal formulations is approximately half that of DMSO-curcumin (Table 3).

In KHOS and MCF-7, cytotoxic effects of liposomal curcumin were 2 to 4 times stronger than those observed in non-liposomal formulations. As expected, the exposure to the phospholipids alone (empty liposomes) does not show any toxic effects in all cell lines. This study showed that all cell lines without the use of liposomes can tolerate about 20  $\mu$ g/ml of curcumin, but the use of liposomes significantly enhances the efficiency of delivery with KHOS and MCF-7.

### Curcumin induced apoptosis and autophagy in vitro

A cell that is undergoing apoptosis demonstrates morphological changes that include cell shrinkage, membrane blebbing, nuclear condensation and DNA fragmentation.<sup>30</sup> The arrows in the phase contrast images (Figure 3, C and D) indicate the formation of blebs and apoptotic bodies in liposomal curcumin-treated KHOS cells. Nuclear condensation and DNA fragmentation can be detected by staining with Hoechst 33342 for fluorescence microscopy.<sup>31</sup> In our study Hoechst staining images (Figure 3, Panels *G* and *H*) illustrate prominent chromatin condensation and apoptotic bodies in liposomal curcumin-treated KHOS as indicated. In control cells and DMSO-curcumin-treated cells, chromatin condensation was not observed (Figure 3, Panels *E* and *F*, respectively). This indicates that DMSO-curcumin induces cell death by a mechanism other than apoptosis. To investigate the cell-death pathway followed by DMSO-curcumin treated cells, we carried out beclin-1 immunocytochemistry. Beclin-1 is the first identified tumor-suppressor protein that functions in the lysosomal degradation pathway of autophagy.<sup>32</sup> In our study we found that beclin-1 levels were markedly increased after 48 hours of DMSO-curcumin treatment and beclin-1 was localized in the perinuclear space as in Figure 4, B, typical of autophagic cells. The expression of beclin-1 was absent in liposomal curcumin-treated cells in Panel C and D.

### Detection of cleaved caspases and cleaved PARP

Caspases, a family of cysteine acid proteases, are cleaved following proteolytic activation in early apoptosis. Cleaved caspases activate other caspases or cleave other key cellular proteins such as Poly (ADP-ribose) polymerase (PARP).<sup>33</sup> The cleavage of PARP into 2 fragments, 89 and 24 kDa, is considered indicative of functional caspase activation.<sup>34</sup> The essential substrate cleaved by both caspase-3 and caspase-7 is PARP. The presence of cleaved PARP is a commonly used diagnostic tool for the detection of apoptosis.<sup>35</sup> The western blot results in Figure 5 show the expression of such apoptotic markers in the lanes with curcumin-liposomes-treated KHOS. Cleaved caspases and cleaved PARP were not observed in lane 1 containing lysate of untreated cells. KHOS displayed a dose-dependent (from 0 to 10 µg/ml) increase in caspase-3, caspase-7, PARP and their cleaved forms. The housekeeping protein, β-actin, used as a loading control, shows expression in all lanes.

### Liposomal curcumin induces apoptosis in OS xenograft model

Human OS tumor was grown in immunocompromised *nu/nu* mice and treated with conventional, HPγCD-curcumin liposomes and empty liposomes as control. Hematoxylin-eosin staining and DeadEnd™ Colorimetric TUNEL (Terminal deoxynucleotidyl transferase dUTP nick end labeling) assay were performed to evaluate the cell-death mechanism in vivo. Figure 6, A shows dark blue hematoxylin-stained nuclei and pink eosin-stained cytoplasm, whereas liposomal curcumin-treated tumors (Figure 6, C and E) shows loss of nuclei in dead cells as indicated by the black arrow. This indicates cell death induced by both the curcumin liposomes. DeadEnd™ Colorimetric TUNEL assay detects DNA fragmentation caused by apoptosis. The terminal deoxynucleotidyl transferase recognizes fragmented nuclei in apoptotic cells and catalyzes addition of deoxynucleotides at the 3' end of DNA.<sup>31</sup> The arrows in Figure 6, D and F show the significant amount of apoptosis (brown spots) in comparison with 6B. The brown spots indicate the apoptotic area with DNA fragmentation.



Thus immunohistochemical assays of the tumor sections showed a significant increase in the apoptotic cells in the tumors treated with liposomal curcumin corroborating in vitro data described in Figure 3.

## Discussion

Therapeutic properties of curcumin have been the topic of several studies involving methods for treating inflammatory disorders,<sup>36</sup> cardiovascular diseases,<sup>37</sup> cancer and other disorders. One of the major drawbacks of using curcumin has been its poor bioavailability presumably because of aqueous solubility and stability in gastrointestinal fluids. This poor bioavailability leads to multiple studies to develop novel drug-delivery approaches, including microemulsions, nanoemulsions, liposomes, solid lipid NPs, microspheres, solid dispersion, polymeric NPs, and self-microemulsifying drug-delivery systems to enhance the bioavailability and therapeutic ability of curcumin.<sup>38</sup> These attempts have revealed promising results for enhanced bioavailability and targeting certain diseases, but there is a gap in the specific tissue targeting of curcumin. Of all the options, DCL preparation is becoming a preferred choice for the delivery of the lipophilic, photolabile and hydrolysis-sensitive drugs. It has been already reported that DCL preparations increase the encapsulation of many hydrophobic drugs, such as ketoprofen, betamethasone and riboflavin.<sup>15,22,39,40</sup> In our study it is clear from the cryo-TEM that all liposomes are spherical and well formed. In experimental variations, it is difficult to state clearly that there is a clear distinction in liposome size between the various formulations. From DLS and cryo-TEM data, it is clear that the inclusion of CD does not change the size of the liposomal NP significantly. Both DLS and cryo-TEM are methods to analyze liposome size and structure, but differences in the analysis with DLS typically measuring mean sizes are larger than those obtained through cryo-TEM. This is a consequence of the enhanced scattering from the minimal number of aggregated liposomes that are present even at the high dilutions used in DLS experiments.<sup>41,42</sup> Further information on the details of the DLS and cryo-TEM analysis is given in the Supplementary Materials section.

The data described in Table 3 demonstrates that liposomal curcumins are significantly more effective than all other formulations in affecting cell viability for the KHOS OS cell line model. On the other hand, normal cells from the same mesenchymal tissue origin (MSCs) retained about 85% cell viability at liposomal curcumin concentrations lethal for KHOS, which is an indicator of the relative low toxicity of these liposomes on normal human cells. Although the KHOS IC<sub>50</sub> values for both liposomal formulations based on curcumin levels are similar, the amount of HP $\gamma$ CD-curcumin liposomes required to reach the effective curcumin level is 2 – 3 times lower than that needed using conventional liposomes simply because of the high curcumin encapsulation efficiency of HP $\gamma$ CD-curcumin liposomes. The same explanation applies to the IC<sub>50</sub> values of liposomal curcumin against MCF-7. Hence the advantage of the CD-based formulation is the lower levels of liposomes that are needed to attain the same therapeutic effect. This circumstance is clearly due to an increased drug-loading capacity for the same amount of phospholipid used in preparing liposomes. RFOS is a slow expanding OS cell line with growth rates half that of KHOS and may possess resistance against liposomal curcumin due to a low uptake as indicated earlier that the rate of uptake directly related to metabolic state of the cell.<sup>43</sup> Although HP $\gamma$ CD has been used in

studies related to the delivery of hydrophobic drugs,<sup>44,45</sup> our study showed both its effectiveness with curcumin and the added effectiveness of packaging the complex in a liposomal delivery system.

The mode of cell death in response to chemotherapeutic drugs may be necrosis, apoptosis or autophagy.<sup>46</sup> Activated immune-response after cell death is one of the major issues associated with chemotherapy-induced cell death. Recently, autophagy has been a point of intense debate in cancer treatment due to its dimorphic roles in cancer development and therapy.<sup>47</sup> It has both tumor-inhibitory and tumor-protective effects.<sup>48</sup> Cell death followed by autophagy could lead to increased immune response. Therefore, drugs that induce apoptosis are desired because they yield least amount of immune response following cell death. Among the 4 curcumin formulations tested, only liposomal formulations induced apoptosis. Although free drug (DMSO-curcumin) was cytotoxic, lack of apoptotic potential suggested cell death either by necrosis or by autophagy. The analysis of autophagy by beclin-1 expression confirmed the autophagic cell death in DMSO-curcumin-treated KHOS cells. Previous, reports have shown curcumin induced cell death by both autophagy and apoptosis.<sup>49</sup> Our results add further information on how curcumin induces autophagy and apoptosis in different formulations. In summary, CD complexation enhances curcumin solubilization and increases entrapment of curcumin in the aqueous liposomal phase. To our knowledge, this is the first report demonstrating the anticancer activity of liposomal curcumin and DCL preparations against OS. Among the cell lines studied, KHOS and MCF-7 were found to be the most sensitive to curcumin delivery in the concentration range 4 – 28 µg/ml of curcumin. DMSO-curcumin induces autophagy, whereas liposomal curcumin induces apoptosis in KHOS.

Curcumin has been extensively tested and approved by the National Institute of Health for Phase I & II clinical trials.<sup>50</sup> These findings, along with the in vivo study described in this article, support the application of curcumin liposomes at the clinical level. Our results indicate liposomal curcumin's anticancer potential against cancer of epithelial as well as mesenchymal origin. Further investigation is needed in additional cell lines of mesenchymal and epithelial origin to understand the liposomal curcumin's anticancer potential against a wide range of tumors.

## Supplementary Material

Refer to Web version on PubMed Central for supplementary material.

## Acknowledgments

We would like to acknowledge Mary Price from Louisiana Cancer Research Consortium FACS Core.

This research was supported by the Louisiana Cancer Research Consortium and the Louisiana Gene Therapy Research Consortium for RP. VJ gratefully acknowledges support from the National Institutes of Health (grant 1RO1EB006493-01).

## Appendix A. Supplementary data

Supplementary data to this article can be found online at doi:10.1016/j.nano.2011.07.011.

## References

1. Shishodia S, Chaturvedi MM, Aggarwal BB. Role of curcumin in cancer therapy. *Curr Probl Cancer*. 2007; 31:243–305. [PubMed: 17645940]
2. Ravindran J, Prasad S, Aggarwal B. Curcumin and cancer cells: how many ways can curry kill tumor cells selectively? *The AAPS J*. 2009; 11:495–510. [PubMed: 19590964]
3. Ghoneim A. Effects of curcumin on ethanol-induced hepatocyte necrosis and apoptosis: implication of lipid peroxidation and cytochrome c. *Naunyn-Schmiedeberg's Arch Pharmacol*. 2009; 379:47–60. [PubMed: 18716759]
4. Kunwar A, Barik A, Mishra B, Rathinasamy K, Pandey R, Priyadarsini KI. Quantitative cellular uptake, localization and cytotoxicity of curcumin in normal and tumor cells. *Biochim Biophys Acta (G)*. 2008; 1780:673–9.
5. Kaminaga Y, Nagatsu A, Akiyama T, Sugimoto N, Yamazaki T, Maitani T, et al. Production of unnatural glucosides of curcumin with drastically enhanced water solubility by cell suspension cultures of *catharanthus roseus*. *FEBS Lett*. 2003; 555:311–6. [PubMed: 14644434]
6. Priyadarsini KI. Photophysics, photochemistry and photobiology of curcumin: Studies from organic solutions, bio-mimetics and living cells. *J Photochem Photobiol C: Photochemistry Reviews*. 2009; 10:81–95.
7. Lan L, Fadi SB, Razelle K. Liposome-encapsulated curcumin. *Cancer*. 2005; 104:1322–31. [PubMed: 16092118]
8. Wang D, Veena MS, Stevenson K, Tang C, Ho B, Suh JD, et al. Liposome-encapsulated curcumin suppresses growth of head and neck squamous cell carcinoma in vitro and in xenografts through the inhibition of nuclear factor  $\kappa$ b by an akt-independent pathway. *Clin Cancer Res*. 2008; 14:6228–36. [PubMed: 18829502]
9. Li L, Ahmed B, Mehta K, Kurzrock R. Liposomal curcumin with and without oxaliplatin: Effects on cell growth, apoptosis, and angiogenesis in colorectal cancer. *Mol Cancer Ther*. 2007; 6:1276–82. [PubMed: 17431105]
10. Kunwar A, Barik A, Pandey R, Priyadarsini KI. Transport of liposomal and albumin loaded curcumin to living cells: an absorption and fluorescence spectroscopic study. *Biochim Biophys Acta (G)*. 2006; 1760:1513–20.
11. Hamre MR, Severson RK, Chuba P, Lucas DR, Thomas RL, Mott MP. Osteosarcoma as a second malignant neoplasm. *Radiother Oncol*. 2002; 65:153–7. [PubMed: 12464443]
12. Lisa M, Rebecca JT, Sharon AS. International osteosarcoma incidence patterns in children and adolescents, middle ages and elderly persons. *Int J Cancer*. 2009; 125:229–34. [PubMed: 19330840]
13. Walters D, Muff R, Langsam B, Born W, Fuchs B. Cytotoxic effects of curcumin on osteosarcoma cell lines. *Inves New Drugs*. 2008; 26:289–97.
14. McCormack B, Gregoriadis G. Drugs-in-cyclodextrins-in liposomes: A novel concept in drug delivery. *Int J Pharm*. 1994; 112:249–58.
15. Loukas YL, Vraka V, Gregoriadis G. Drugs, in cyclodextrins, in liposomes: A novel approach to the chemical stability of drugs sensitive to hydrolysis. *Int J Pharm*. 1998; 162:137–42.
16. Perrault SD, Walkey C, Jennings T, Fischer HC, Chan WC. Mediating tumor targeting efficiency of nanoparticles through design. *Nano Lett*. 2009; 9:1909–15. [PubMed: 19344179]
17. DeComas AM, Penfornis P, Harris MR, Meyer MS, Pochampally RR. Derivation and characterization of an extra-axial chordoma cell line (each-1) from a scapular tumor. *J Bone Joint Surg Am*. 2010; 92:1231–40. [PubMed: 20439670]
18. Thangapazham RL, Puri A, Tele S, Blumenthal R, Maheshwari RK. Evaluation of a nanotechnology based carrier for delivery of curcumin in prostate cancer cells. *Int J Oncol*. 2008; 32:1119–23. [PubMed: 18425340]
19. Tønnesen HH, Måsson M, Loftsson T. Studies of curcumin and curcuminoids. Xxvii. Cyclodextrin complexation: solubility, chemical and photochemical stability. *Int J Pharm*. 2002; 244:127–35. [PubMed: 12204572]

20. Xu P, Tan G, Zhou J, He J, Lawson LB, McPherson GL, et al. Undulating tubular liposomes through incorporation of a synthetic skin ceramide into phospholipid bilayers. *Langmuir*. 2009; 25:10422–5. [PubMed: 19694462]
21. Chithrani DB, Dunne M, Stewart J, Allen C, Jaffray DA. Cellular uptake and transport of gold nanoparticles incorporated in a liposomal carrier. *Nanomedicine*. 2010; 6:161–9. [PubMed: 19447206]
22. Maestrelli F, González-Rodríguez ML, Rabasco AM, Mura P. Preparation and characterisation of liposomes encapsulating ketoprofen-cyclodextrin complexes for transdermal drug delivery. *Int J Pharm*. 2005; 298:55–67. [PubMed: 15941634]
23. Shaikh J, Ankola DD, Beniwal V, Singh D, Kumar MN. Nanoparticle encapsulation improves oral bioavailability of curcumin by at least 9-fold when compared to curcumin administered with piperine as absorption enhancer. *Eur J Pharm Sci*. 2009; 37:223–30. [PubMed: 19491009]
24. Lal A, Pan Y, Navarro F, Dykxhoorn DM, Moreau L, Meire E, et al. Mir-24-mediated downregulation of h2ax suppresses DNA repair in terminally differentiated blood cells. *Nat Struct Mol Biol*. 2009; 16:492–8. [PubMed: 19377482]
25. Selassie CD, Kapur S, Verma RP, Rosario M. Cellular apoptosis and cytotoxicity of phenolic compounds: a quantitative structure–activity relationship study. *J Med Chem*. 2005; 48:7234–42. [PubMed: 16279782]
26. Shin HC, Alani AW, Rao DA, Rockich NC, Kwon GS. Multi-drug loaded polymeric micelles for simultaneous delivery of poorly soluble anticancer drugs. *J Control Release*. 2009; 140:294–300. [PubMed: 19409432]
27. Gregorc A, Ellis JD. Cell death localization in situ in laboratory reared honey bee (*Apis mellifera* L.) larvae treated with pesticides. *Pest Biochem Physiol*. 2011; 99:200–7.
28. Singh R, Tønnesen H, Vogensen S, Loftsson T, Másson M. Studies of curcumin and curcuminoids. The stoichiometry and complexation constants of cyclodextrin complexes as determined by the phase-solubility method and uv–vis titration. *J Incl Phenom Macrocycl Chem*. 2010; 66:335–48.
29. Moreno-Sánchez R, Rodríguez-Enríquez S, Marín-Hernández A, Saavedra E. Energy metabolism in tumor cells. *FEBS J*. 2007; 274:1393–418. [PubMed: 17302740]
30. Lane JD, Allan VJ, Woodman PG. Active relocation of chromatin and endoplasmic reticulum into blebs in late apoptotic cells. *J Cell Sci*. 2005; 118:4059–71. [PubMed: 16129889]
31. Darzynkiewicz Z, Galkowski D, Zhao H. Analysis of apoptosis by cytometry using tunel assay. *Methods*. 2008; 44:250–4. [PubMed: 18314056]
32. Li Z, Chen B, Wu Y, Jin F, Xia Y, Liu X. Genetic and epigenetic silencing of the beclin 1 gene in sporadic breast tumors. *BMC Cancer*. 2010; 10:98. [PubMed: 20230646]
33. Matas D, Juknat A, Pietr M, Klin Y, Vogel Z. Anandamide protects from low serum-induced apoptosis via its degradation to ethanolamine. *J Biol Chem*. 2007; 282:7885–92. [PubMed: 17227767]
34. Bressnot A, Marchal S, Bezdetnaya L, Garrier J, Guillemin F, Plenat F. Assessment of apoptosis by immunohistochemistry to active caspase-3, active caspase-7, or cleaved parp in monolayer cells and spheroid and subcutaneous xenografts of human carcinoma. *J Histochem Cytochem*. 2009; 57:289–300. [PubMed: 19029405]
35. Carter R, Sykes V, Lanning D. Scarless fetal mouse wound healing may initiate apoptosis through caspase 7 and cleavage of PARP. *J Surg Res*. 2009; 156:74–9. [PubMed: 19555972]
36. Lubbad A, Oriowo M, Khan I. Curcumin attenuates inflammation through inhibition of TLR-4 receptor in experimental colitis. *Mol Cell Biochem*. 2009; 322:127–35. [PubMed: 19002562]
37. Wongcharoen W, Phrommintikul A. The protective role of curcumin in cardiovascular diseases. *Int J Cardiol*. 2009; 133(2):145–51. [PubMed: 19233493]
38. Kumar A, Ahuja A, Ali J, Baboota S. Conundrum and therapeutic potential of curcumin in drug delivery. *Crit Rev Ther Drug Carrier Syst*. 2010; 27:279–312. [PubMed: 20932240]
39. Piel G, Piette M, Barillaro V, Castagne D, Evrard B, Delattre L. Betamethasone-in-cyclodextrin-in-liposome: the effect of cyclodextrins on encapsulation efficiency and release kinetics. *Int J Pharm*. 2006; 312:75–82. [PubMed: 16455215]

40. Loukas YL, Jayasekera P, Gregoriadis G. Characterization and photoprotection studies of a model gamma-cyclodextrin included photolabile drug entrapped in liposomes incorporating light absorbers. *J Phys Chem.* 1995; 99:11035–40.
41. Holzer M, Barnert S, Momm J, Schubert R. Preparative size exclusion chromatography combined with detergent removal as a versatile tool to prepare unilamellar and spherical liposomes of highly uniform size distribution. *J Chromatogra A.* 2009; 1216:5838–48.
42. Crawford R, Dogdas B, Keough E, Haas RM, Wepukhulu W, Krotzer S, et al. Analysis of lipid nanoparticles by Cryo-EM for characterizing siRNA delivery vehicles. *Int J Pharm.* 2011; 403(1–2):237–44. [PubMed: 20974237]
43. Daleke DL, Hong K, Papahadjopoulos D. Endocytosis of liposomes by macrophages: Binding, acidification and leakage of liposomes monitored by a new fluorescence assay. *Biochim Biophys Acta Biomembr.* 1990; 1024:352–66.
44. Hegge AB, Schuller RB, Kristensen S, Tonnesen HH. In vitro release of curcumin from vehicles containing alginate and cyclodextrin. *Studies of curcumin and curcuminoides.* *Pharmazie.* 2008; 63:585–92. [PubMed: 18771007]
45. Rasheed A, Ashok Kumar CK, Sravanthi VVNSS. Cyclodextrins as drug carrier molecule: a review. *Sci Pharm.* 2008; 76:567–98.
46. Shao Y, Gao Z, Marks PA, Jiang X. Apoptotic and autophagic cell death induced by histone deacetylase inhibitors. *PNAS U S A.* 2004; 101:18030–5.
47. Hippert MM, O'Toole PS, Thorburn A. Autophagy in cancer: good, bad, or both? *Cancer Res.* 2006; 66:9349–51. [PubMed: 17018585]
48. Gozuacik D, Kimchi A. Autophagy as a cell death and tumor suppressor mechanism. *Oncogene.* 2004; 23:2891–906. [PubMed: 15077152]
49. Aoki H, Takada Y, Kondo S, Sawaya R, Aggarwal BB, Kondo Y. Evidence that curcumin suppresses the growth of malignant gliomas in vitro and in vivo through induction of autophagy: role of Akt and extracellular signal-regulated kinase signaling pathways. *Mol Pharmacol.* 2007; 72:29–39. [PubMed: 17395690]
50. ClinicalTrials.gov. US National Institutes of Health. Available from: [www.clinicaltrials.gov/ct2/results?term=curcumin](http://www.clinicaltrials.gov/ct2/results?term=curcumin). Accessed August 31, 2011

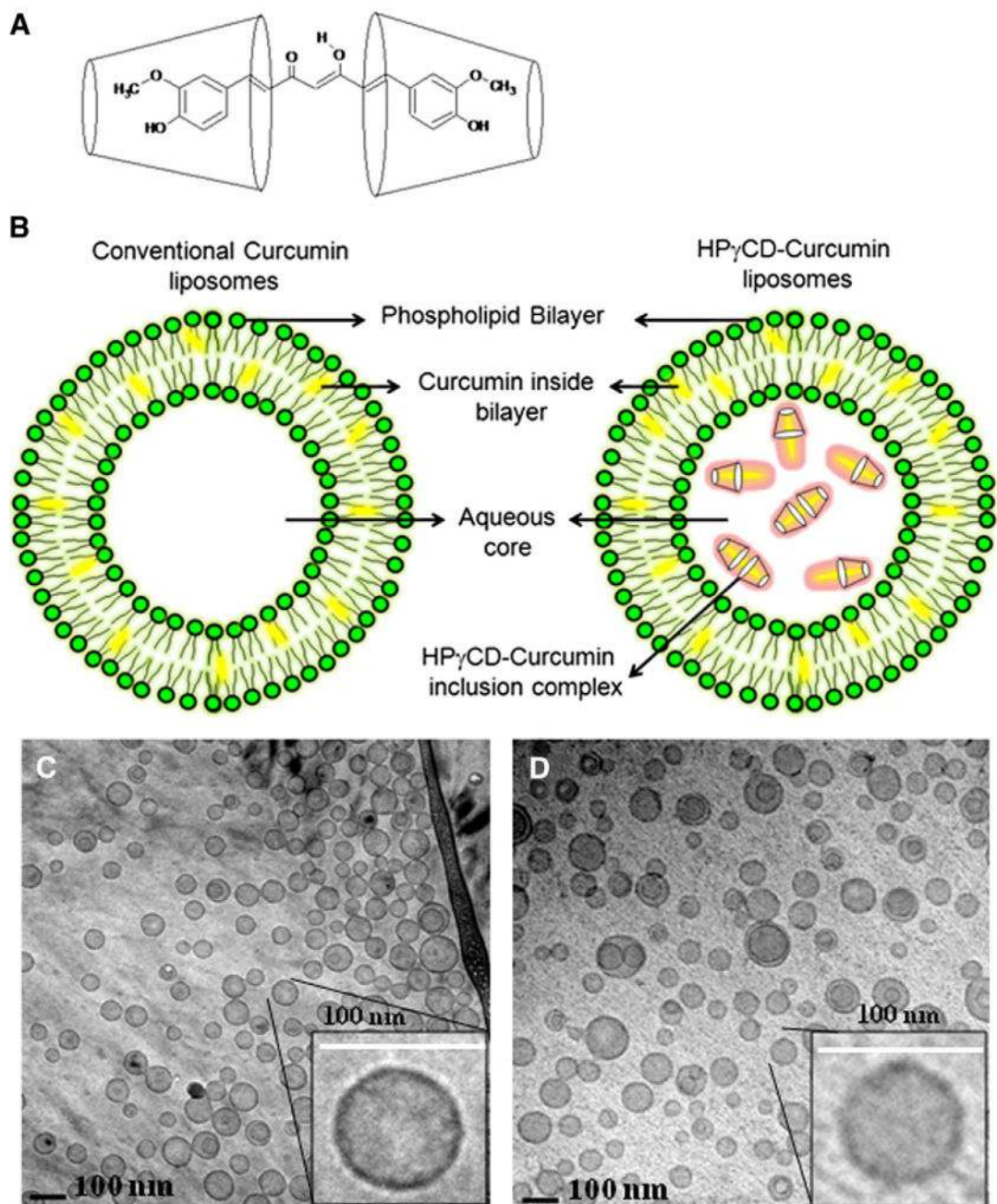


**Figure 1.** Liposomal curcumin formulations and cryo-TEM images (**A**) 2:1 complex of HP $\gamma$ CD and curcumin (**B**) Schematic representation of conventional and HP $\gamma$ CD-curcumin liposomes (**C**) Conventional curcumin liposomes, (**D**) HP $\gamma$ CD-curcumin liposomes. All the scale bars represent 100 nm.

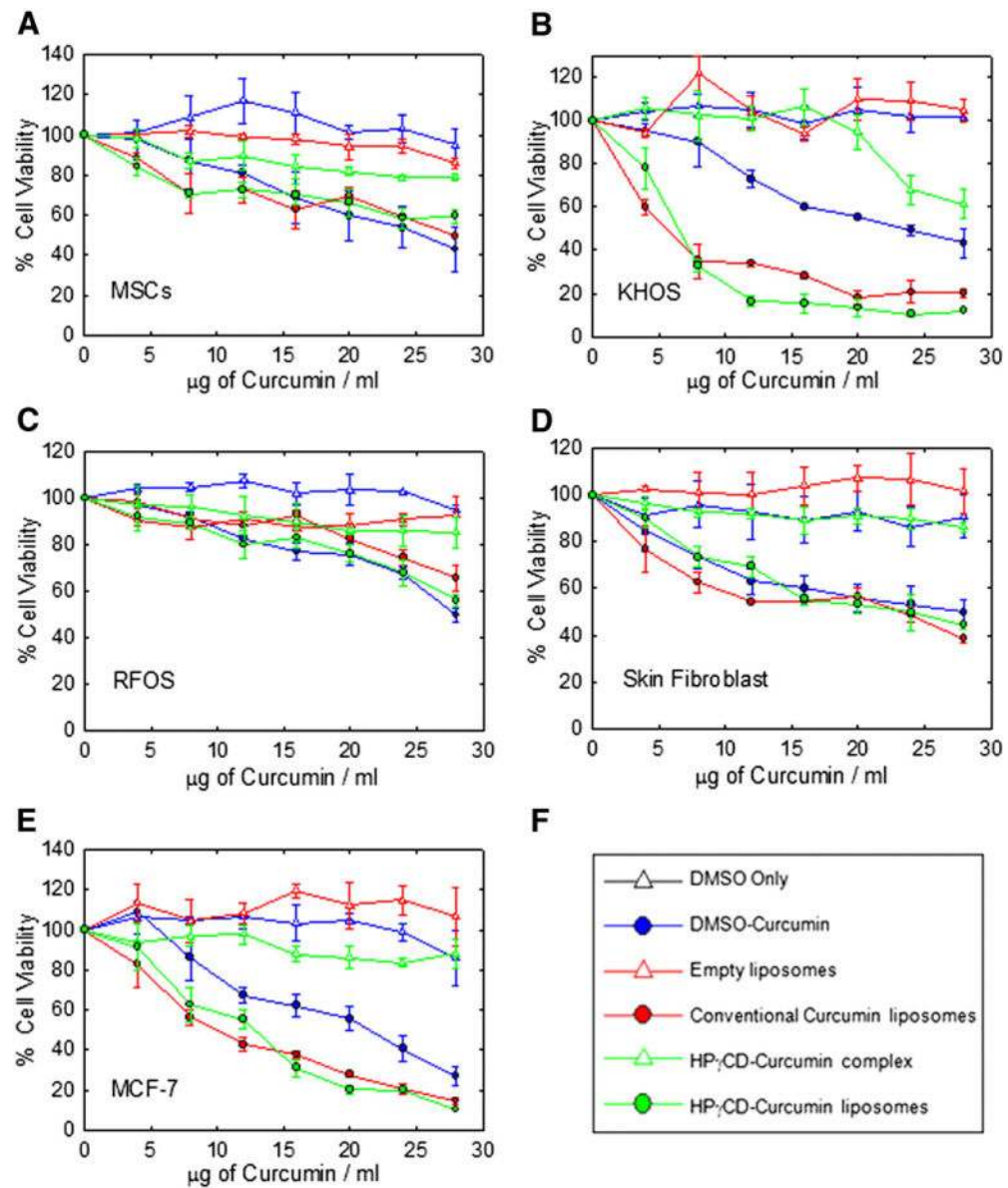


**Figure 2.** Effect of different curcumin formulations on cell lines of mesenchymal and epithelial origin. (A) Human mesenchymal stem cells (B) KHOS (C) RFOS (D) Skin fibroblast (E) MCF-7 (F) Legends. Values represent the mean  $\pm$  SD of triplicate experiments after 48 h of exposure to different curcumin formulations.

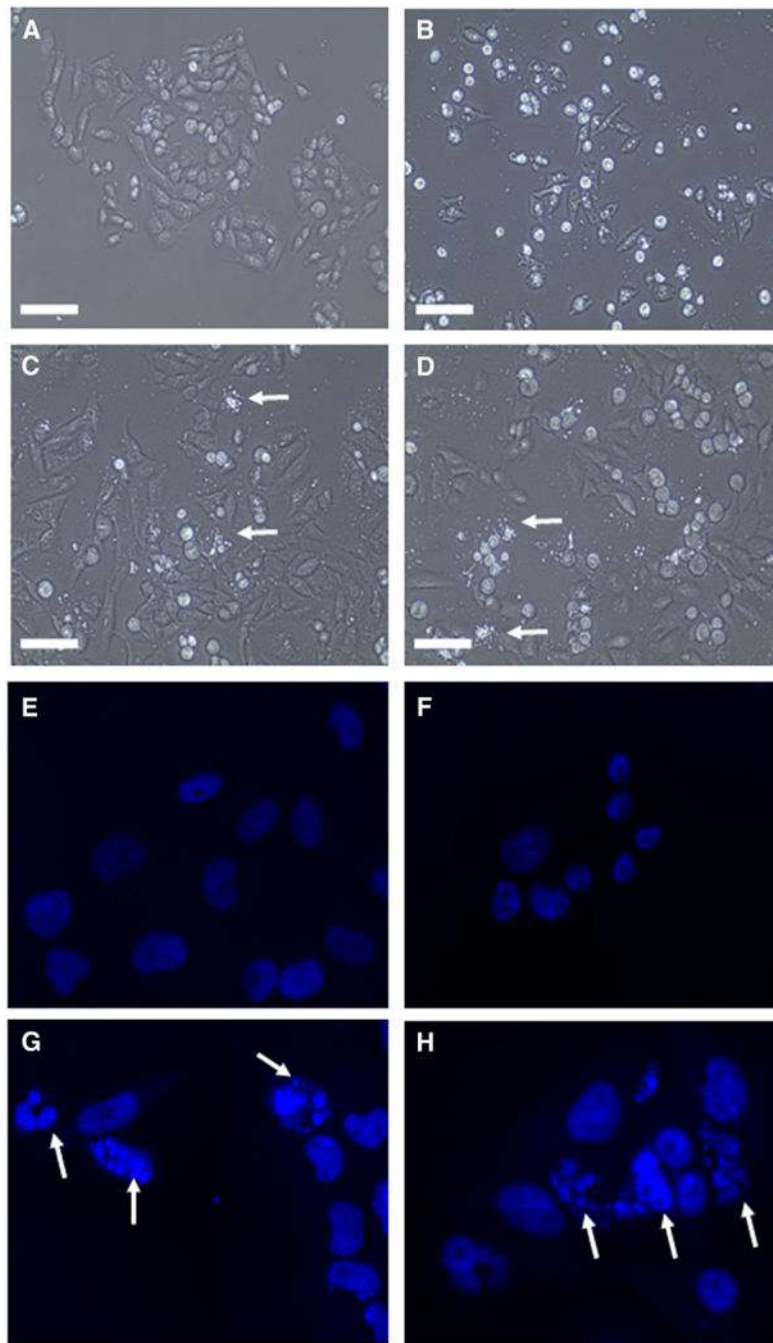


**Figure 3.** Phase contrast and Hoechst staining images of curcumin treated KHOS cells. (A, E) Empty liposomes (B, F) DMSO-curcumin (C, G) Conventional curcumin liposomes (D, H) HP $\gamma$ CD-curcumin liposomes. Cells treated with respective curcumin formulations at IC<sub>50</sub>. White arrows point to apoptotic bodies in panel C, D, G and H. Scale bar in phase contrast images (A to D) represents 100  $\mu$ m and Hoechst staining images (E to H) were taken at magnification of 600 $\times$ .



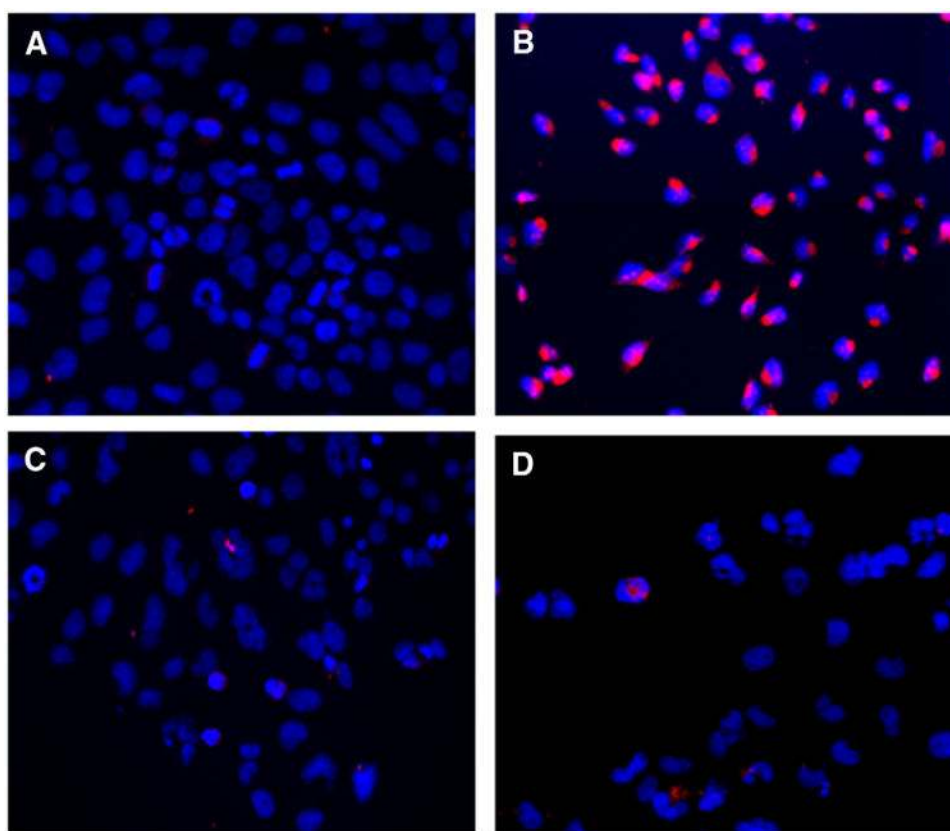


**Figure 4.** DMSO-curcumin induces autophagy. KHOS OS cell line was treated in (A) Empty liposomes (B) DMSO-curcumin (C) liposomal curcumin (D) HP $\gamma$ CD-curcumin liposomes. Cells treated with respective curcumin formulations at IC<sub>50</sub>. Nuclei in blue (Hoechst 33342 staining) and beclin-1 expression in red (Immunocytochemistry with AlexaFluor 555). Magnification – 200 $\times$ .

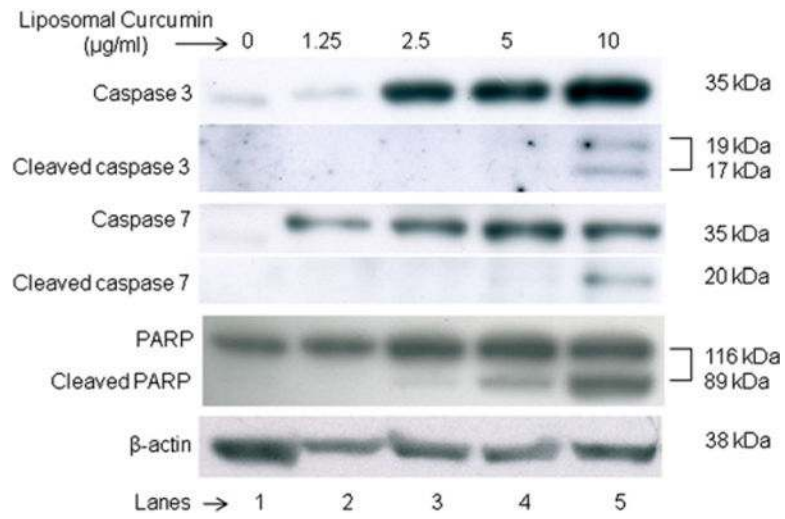


**Figure 5.** Western blot illustrating expression of apoptotic markers in KHOS cells treated with liposomal curcumin. Expression of caspase cascade components (caspase 3, 7 and PARP) was found to increase with the concentration of liposomal curcumin. Lane 1 is control, Lane 2 to 5 indicate liposomal curcumin-treated cells at different concentration.

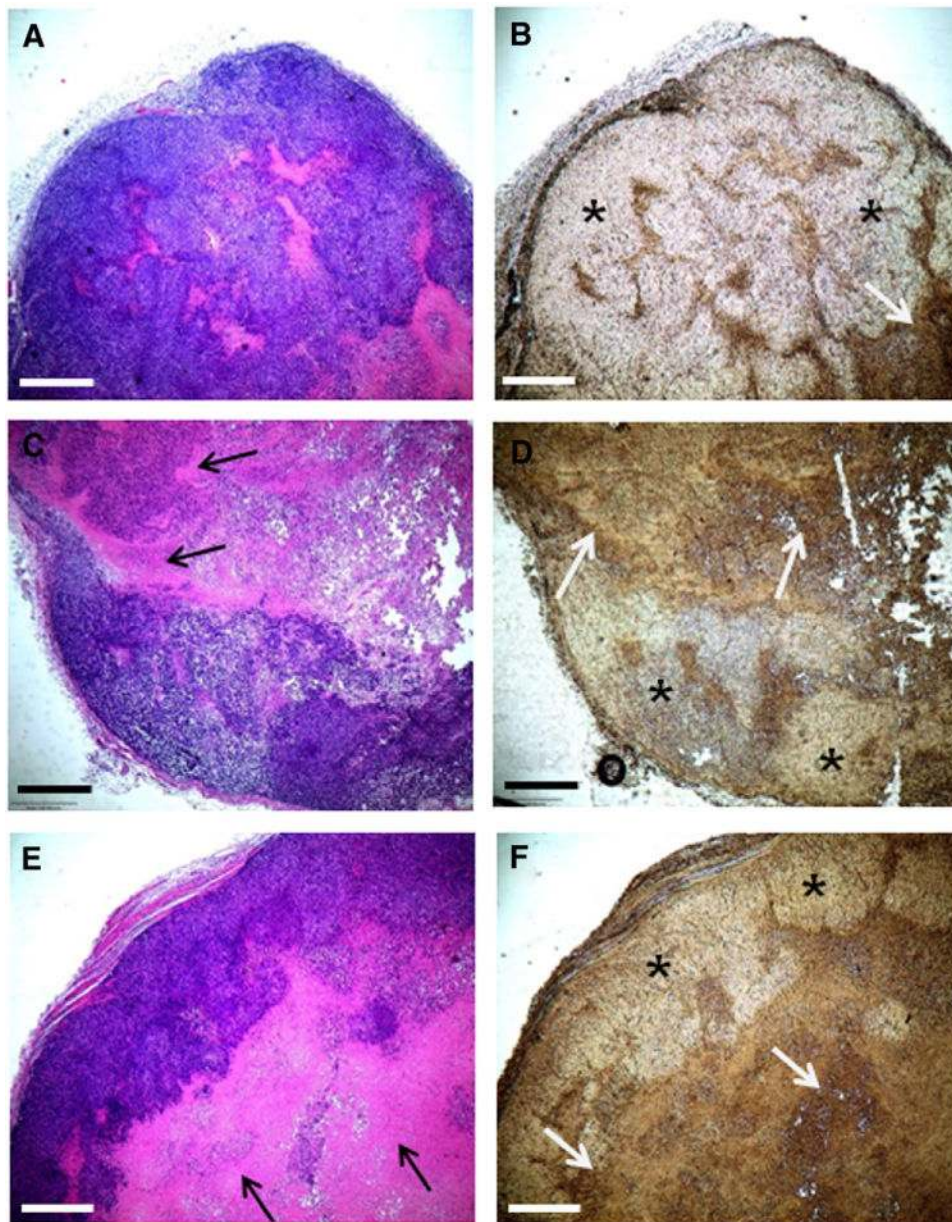


**Figure 6.** Curcumin liposomes induce apoptotic cell death in OS xenograft model. Tumors treated with empty liposomes (**A**) and (**B**), with conventional curcumin liposomes (**C**) and (**D**) and with HP $\gamma$ CD-curcumin liposomes (**E**) and (**F**). Subfigures A, C, E represent hematoxylin and eosin staining for histopathology of tumor, whereas B, D, F are the images of TUNEL staining for detection of apoptosis. (\* indicates high proliferative area and white arrows indicate apoptotic area). All the scale bars indicate 500  $\mu$ m.

**Table 1**

Size distribution analysis of liposomal formulations by DLS and Cryo-TEM

Formulation	DLS Data		Cryo-TEM Data			
	Diameter (nm)	SD	SE	Diameter (nm)	Half Width (SD)	SE
Conventional curcumin liposomes	104.7	23.1	0.9	71	20	1.38
HP $\gamma$ CD-curcumin liposomes	98.2	30.1	0.7	67	16	2.35

**Table 2**

Percent encapsulation efficiency in terms of total curcumin used in liposome preparation

<b>Curcumin in</b>	<b>Conventional curcumin liposomes (CD-free)</b>	<b>2.5% HP<math>\gamma</math>CD-curcumin liposomes</b>
Liposome Only	0.8 mg/ml	1.3 mg/ml
Supernatant Only	0 mg/ml	0.7 mg/ml
Curcumin encapsulated	0.8 mg/ml	1.3 mg/ml
Total curcumin encapsulated in 5 ml	4 mg	6.5 mg
Total curcumin used	13 mg	13 mg
% Encapsulation of starting curcumin	30.7	50

Author Manuscript

Author Manuscript

Author Manuscript

Author Manuscript

**Table 3**Inhibitory concentration (IC<sub>50</sub> in µg/ml) of curcumin formulations

Cell line	DMSO- curcumin	Conventional curcumin liposomes	HPγCD- curcumin liposomes
KHOS	22.8 ± 1.9	5.4 ± 0.9	6.4 ± 0.7
MCF-7	20 ± 1.8	10.2 ± 0.8	11.5 ± 1.1
Skin fibroblast	27 ± 5	20 ± 3.5	22 ± 2.1

IC<sub>50</sub> – Concentration necessary to inhibit 50% of cell growth.

Author Manuscript

Author Manuscript

Author Manuscript

Author Manuscript